PROTON–PROTON INTENSITY INTERFEROMETRY: SPACE–TIME STRUCTURE OF THE EMITTING ZONE IN Ni+Ni COLLISIONS*

M. KOROLIJA[a,b], D. SHAPIRA[b] AND N. CINDRO[a]

[a]Physics Department, Ruder Bošković Institute
10001 Zagreb, Croatia

[b]Physics Division, Oak Ridge National Laboratory
Oak Ridge, TN 37830, USA

(Received December 8, 1995)

A brief description is given of the Hanbury-Brown–Twiss effect method for determining the space-time structure of the proton-emitting source in a nucleus-nucleus collision. In this context a measurement of exclusive p-p correlations from ^{58}Ni+^{58}Ni at 850 MeV is analyzed. The data served to study the directional dependence of the p-p correlation function and, for the first time, extract separately the source size and the particle-emission time.

PACS numbers: 25.75.Cz

1. Introduction: Interferometry and the Hanbury-Brown–Twiss effect

Interferometry as a method of determining the distance between two small, close-by objects is based on Young's 1801 experiment with two slits acting as two coherent light sources producing an interference pattern on a screen. The distance d between the two slits is related to the wavelength λ and the angle δ_n of the n-th interference maximum by

$$d \cdot \sin(\delta_n) = n\lambda \qquad (n = 1, 2, 3...)\,.$$

Conversely, for a known λ and a measured δ_n, the distance d between two small objects can be determined. This is the basis of the conventional

* Presented at the XXIV Mazurian Lakes School of Physics, Piaski, Poland, August 23–September 2, 1995.

(*amplitude*) interferometry, which was for a long time a standard method for measuring either distances or wavelengths. By 1920 Michelson used it to measure the radius of stars. This astrophysical application was, however, restricted to 7 highest stars only, the limitation being the phase shifts caused by the passage of the stellar light through the atmosphere.

In 1954 two astronomers, Hanbury-Brown and Twiss [1], overcame these difficulties by devising an ingenious interferometric method based on *intensity* (rather than amplitude) interferometry. After the initial measurement of the radius of the lightest star in the sky, Sirius, this method became standard in astrophysical studies.

The original Hanbury-Brown–Twiss (HBT) method consists in measuring the dependence of the correlation function of two photons emitted by a source on their relative momentum:

$$R(\boldsymbol{k}_1, \boldsymbol{k}_2) = \frac{\langle n_{12} \rangle}{\langle n_1 \rangle \langle n_2 \rangle} - 1 \,. \tag{1}$$

Here $\langle n_{12} \rangle$ is the probability for the two photons with momenta $\boldsymbol{k}_1$ and $\boldsymbol{k}_2$ to be detected in detectors 1 and 2 and $\langle n_i \rangle$ is the probability for detecting a photon with momentum $\boldsymbol{k}_i$ in the detector i. The obvious advantage of the HBT method in comparison with the amplitude interferometry is that R is given in counting rates only (no phases!). The underlying physics is that, owing to quantum-statistical properties, the two photons (two identical bosons) display a non-vanishing correlation function for small values of $\Delta \boldsymbol{k}$. The function can be written as

$$R(\boldsymbol{k}_1, \boldsymbol{k}_2) = 2 \cos^2 \left[\tfrac{1}{2} (\boldsymbol{k}_2 - \boldsymbol{k}_1)(\boldsymbol{r}_a - \boldsymbol{r}_b) \right] . \tag{2}$$

The correlation function for the simultaneous emission of two photons from an extended source ($\Delta \boldsymbol{r} = |\boldsymbol{r}_a - \boldsymbol{r}_b| \neq 0$) is obtained by integrating the above equation over the spatial extension of the source. Hence, the possibility of determining its size.

The generalization of the HBT method to other bosons and to fermions and its application to source-size determination in subatomic physics was performed some years later. In 1977 Koonin [2] proposed to use two-proton intensity interferometry to obtain what is now, somewhat pompously, called the "space-time structure" of the reaction (emission) zone formed in the collision of two energetic heavy ions. Compared with photons and pions, there are some advantages in measuring the correlation function of two outgoing protons (detection, the fact that protons are not created in the collision) although they introduce uncertainties in the treatment of the final-state interaction (Coulomb, nuclear effects): All this is to say that the extraction of space-time information on the source from p-p correlation studies is neither simple nor straightforward.

In this contribution we describe the analysis of p-p correlation functions obtained from a triple (two protons and a heavy fragment) coincidence measurement from ^{58}Ni+^{58}Ni collisions at 15 MeV/nucleon.

2. Outline of the experiment

The two-proton correlation function from bombardment of ^{58}Ni+^{58}Ni at 850 MeV was measured at the Holifield Heavy Ion Research Facility of the Oak Ridge National Laboratory using the Heavy-Ion–Light-Ion (HILI) detection system [3]. In this system, which acts as a 4π detector for products of inverse kinematics reactions, triple p-p-*fragment* coincidences were registered, with fragments detected in a position-sensitive ionization chamber and protons in a 96-piece $\Delta E - E$ phoswich scintillator detector array (Fig. 1).

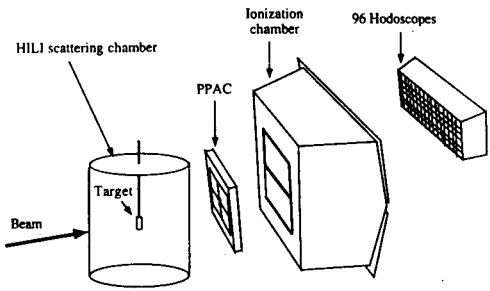

Fig. 1. Schematic view of the HILI (Heavy-Ion–Light-Ion) detection system.

The measurements were performed in two geometries: in geometry I, all the three particles were detected above the beam axis, in geometry II, the fragment was detected below the beam axis. Obviously, stronger correlation effects are expected in geometry I, since only this geometry allows for the measurement of the proton momenta $\boldsymbol{p}_1$ and $\boldsymbol{p}_2$ in a small cone around the fragment's momentum $\boldsymbol{p}_f$.

An important feature of the present analysis is the gating on the relative velocity

$$v_{\mathrm{rel}} = |\boldsymbol{v}_{pp} - \boldsymbol{v}_f| \,, \tag{3}$$

with $\boldsymbol{v}_{pp}$ the velocity of the center of mass of the two protons and $\boldsymbol{v}_f$ the velocity of the fragment (source). v_{rel} is, thus, the velocity with which the proton pair leaves the source. The transformation of the measured quantity $\boldsymbol{p}_f$ into $\boldsymbol{v}_f$ was performed using the code LILITA [4] for a restricted fragment range $21 \leq Z \leq 26$.

3. Analysis and results

As mentioned in Section 1, the final-state interaction model of Koonin [2] allows the determination of the size r_0 and the lifetime τ of the hot proton emitting zone in a nucleus–nucleus collision as the result of a two-parameter fit. This information is combined in an effective source size

$$\rho = \left[r_0^2 + (v_{\mathrm{rel}} \cdot \tau)^2\right]^{1/2}. \tag{4}$$

The second term in the above expression reflects the propagation of the energy in the colliding system; obviously, $\rho = r_0$ for $\tau = 0$. The procedure is to compare the experimentally obtained correlation function with that calculated from the final-state interaction model [2] and to obtain the best-fit values of the parameters r_0 and $v_{\mathrm{rel}} \cdot \tau$ from Eq. (4). The problem is, however, that owing to the insufficient quality of the data, the analysis has so far been unable to disentangle the spatial from the time information, so that only combinations of values of r_0 and $v_{\mathrm{rel}} \cdot \tau$ could be obtained. Ref. [2], however, brings forth the point that for the same values of the parameters r_0 and τ, there is a difference in the shape of the proton–proton correlation function when one takes (a) $\Delta \boldsymbol{p}$ perpendicular to $\boldsymbol{v}_{\mathrm{rel}}$ and (b) $\Delta \boldsymbol{p}$ parallel to $\boldsymbol{v}_{\mathrm{rel}}$. Following this idea, in this contribution we report on an analysis of triple coincidences from deep inelastic collisions of ^{58}Ni+^{58}Ni at 15 MeV/nucleon where the parameters r_0 and τ were separately deduced from this difference in the p-p correlation functions. Thus this analysis differs from that presented in Ref. [5], where the combined values of the parameters $r)0$ and τ were determined from the v_{rel} dependence of the p-p correlation function. It follows, however, the analysis published recently in Ref. [6].

3.1. The correlation function

As stated in Section 1, the correlation function R is defined as the normalized ratio of the two-particle coincidence cross section to the product of the single-particle cross sections:

$$R(\boldsymbol{p}_1, \boldsymbol{p}_2) + 1 = \frac{\frac{1}{\sigma_{\mathrm{coinc.}}} \frac{d^2\sigma_{\mathrm{coinc.}}}{dp_1 dp_2}}{\left[\frac{1}{\sigma_{\mathrm{singl.}}} \frac{d\sigma_{\mathrm{singl.}}}{dp_1}\right] \left[\frac{1}{\sigma_{\mathrm{singl.}}} \frac{d\sigma_{\mathrm{singl.}}}{dp_2}\right]}. \tag{5}$$

In this expression the two-particle coincidence cross section contains both the correlated and uncorrelated particle pairs, whereas the product of the single-particle cross sections is a function of uncorrelated particles only. Hence the importance of determining a background which will eliminate

uncorrelated pairs. In this contribution the background yield is constructed from the two-particle coincidence yield by mixing particles from different coincidence events [7, 8], rather than constructing it from the product of single-particle yields. Thus, following this method, outlined briefly in Ref. [6], Eq. (5) reads

$$R(\boldsymbol{p}_1,\boldsymbol{p}_2,\boldsymbol{p}_f)+1=C\frac{\sigma_{123}(\boldsymbol{p}_1,\boldsymbol{p}_2,\boldsymbol{p}_f)}{\Sigma_i\Sigma_j\sigma'_{123}(\boldsymbol{p}_{1,i},\boldsymbol{p}_{2,i},\boldsymbol{p}_{f,i};\boldsymbol{p}_{1,j},\boldsymbol{p}_{2,j},\boldsymbol{p}_{f,j})}, \tag{6}$$

where σ_{123} is the measured yield of p-p-*fragment* coincidences of two protons and a fragment with momenta $\boldsymbol{p}_1,\boldsymbol{p}_2$ and $\boldsymbol{p}_f$, respectively, and the background yield σ'_{123} is constructed by mixing protons $\boldsymbol{p}_{1,i}$ and $\boldsymbol{p}_{2,j}$ from events i and j, respectively. Equation (6) is normalized to the calculated $R(\boldsymbol{p}_1,\boldsymbol{p}_2)$ at large Δp through the normalization constant C. Note here that the integration of Eq. (6) over $\boldsymbol{p}_f$ straightforwardly yield Eq. (5).

3.2. The $\Delta p_{\|}$ and $\Delta p_{\perp}$ dependence

As mentioned earlier, within the frame of Ref. [2] and for nonvanishing characteristic emission times τ, the p-p correlation function depends on both Δp, the magnitude of $\Delta\boldsymbol{p}$, and θ_{rel}, the angle between $\Delta\boldsymbol{p}$ and $\boldsymbol{v}_{\mathrm{rel}}$. In Ref. [6] we used this directional dependence of the p-p correlation to independently deduce the two parameters, r_0 and $v_{\mathrm{rel}}\cdot\tau$ present in the model of Ref. [2]. To achieve this goal, the p-p correlation was measured for two limiting cases: (1) $\Delta\boldsymbol{p}$ parallel to $\boldsymbol{v}_{\mathrm{rel}}(\Delta p_{\perp}=0)$ and (2) $\Delta\boldsymbol{p}$ perpendicular to $\boldsymbol{v}_{\mathrm{rel}}(\Delta p_{\|}=0)$. Owing to the limited momentum resolution and the finite number of registered triple coincidences, the above strict conditions were relaxed to $\Delta p_{\perp}$, $\Delta p_{\|}\leq 15$ MeV/c.

The component of the p-p correlation function obtained by imposing $\Delta p_{\perp}\leq 15$ MeV/c is shown in Fig. 2 as open symbols; Fig. 3 shows this for $\Delta p_{\|}\leq 15$ MeV/c. The thick lines in the figures show the p-p correlation functions calculated using the model of Ref. [2] for two different sets of parameters, respectively. As can be seen from the figures, the two sets ($r_0=3$ fm and $v_{\mathrm{rel}}\cdot\tau=10$ fm and $r_0=5$ fm and $v_{\mathrm{rel}}\cdot\tau=3$ fm) describe $r_0=5$ fm and $v_{\mathrm{rel}}\cdot\tau=3$ fm) describe the correlation functions equally well. Thus, to check the sensitivity of the extracted p-p correlations on the chosen values of r_0 and $v_{\mathrm{rel}}\cdot\tau$, a χ^2 defined as

$$\chi^2=\Sigma_i\left[\frac{R_i^{\mathrm{exp}}-R_i^{\mathrm{th}}}{\Delta R_i^{\mathrm{exp}}}\right]^2 \tag{7}$$

was calculated with R_i^{exp} and R_i^{th} the experimental and calculated correlation functions, respectively.

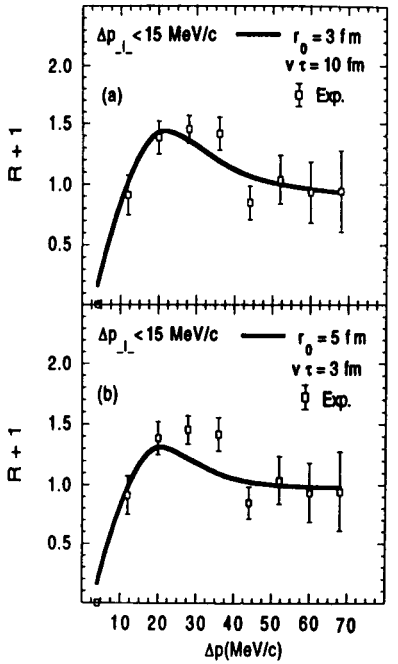

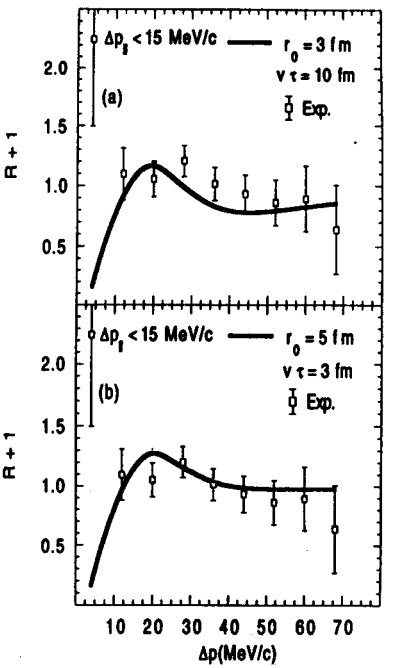

Fig. 2. The measured p-p correlation function for the $\Delta p_\perp \leq 15$ MeV/c cut imposed on the data. The data are shown as open symbols; the thick lines show two different fits to the measured correlation function.

Fig. 3. The same as Fig. 2, but for $\Delta p_\parallel \leq 15$ MeV/c.

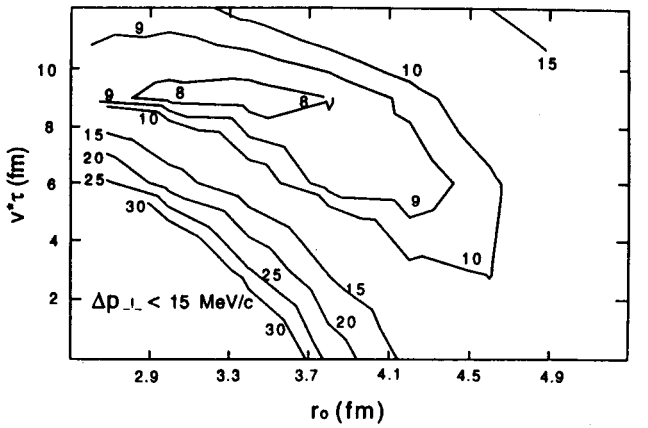

Fig. 4. Contour plots of χ^2 (Eq. (7)) for the $\Delta p_\perp \leq 15$ MeV/c cut imposed on the data.

Fig. 4 shows contour plot representations of the χ^2 values for $\Delta p_\perp \leq 15$ MeV/c and Fig. 5 for $\Delta p_\parallel \leq 15$ MeV/c. The contour plots have been obtained by calculating χ^2 in the range 2.6 fm $\leq r_0 \leq$ 5 fm and 0 fm $\leq v_{\rm rel} \cdot \tau \leq$ 12 fm, in steps of $\Delta r_0 = 0.4$ fm and $\Delta(v_{\rm rel} \cdot \tau) = 3$ fm, respectively.

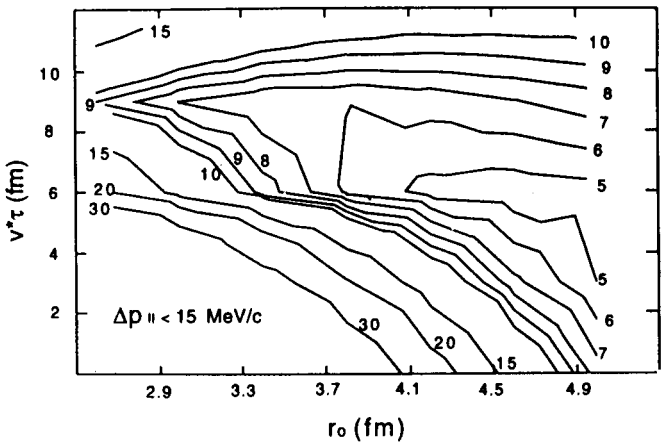

Fig. 5. The same as Fig. 4 but for $\Delta p_\parallel \leq 15$ MeV/c.

Inspection of Fig. 4 reveals a minimum of χ^2 at $r_0 \sim 3.5$ fm and $v_{\rm rel} \cdot \tau \sim 9$ fm. Although less pronounced, a minimum is also visible in Fig. 5 for $r_0 \sim 4.5$ fm and $v_{\rm rel} \cdot \tau \sim 6$ fm. We decided to rely on the χ^2 analysis in Fig. 4 and take the ranges

$$r_0 = 3.3^{+1.3}_{-0.7} \text{ fm (Gaussian density) and} \tag{7a}$$

$$v_{\rm rel} \cdot \tau = 9^{+3}_{-1} \text{ fm} \tag{7b}$$

as the final values of the extracted parameters r_0 and $v_{\rm rel} \cdot \tau$. Transforming the Gaussian into a uniform density, we obtain $r_0 = 5.2^{+2.0}_{-1.1}$ fm, in reasonable agreement with the known sizes of deep inelastic fragments (Ni-like nuclides).

The data allow a fairly safe estimate of the half-life of the source by replacing $v_{\rm rel}$ by its most probable value $\langle v_{\rm rel} \rangle$. The measured $\langle v_{\rm rel}/c \rangle$ distributions for the two cuts are shown in Figs. 6a,b, respectively. A Gaussian fit to these distributions gives $\langle v_{\rm rel}/c \rangle = 0.11$ in both cases. Combining it with the obtained value of $v_{\rm rel} \cdot \tau$, one obtains

$$\tau \approx (3.2 \pm 1.5) \times 10^{-22} \text{s}. \tag{7c}$$

This value of the emission time τ fits well within the recently deduced nucleon emission times of highly excited composite nuclei.

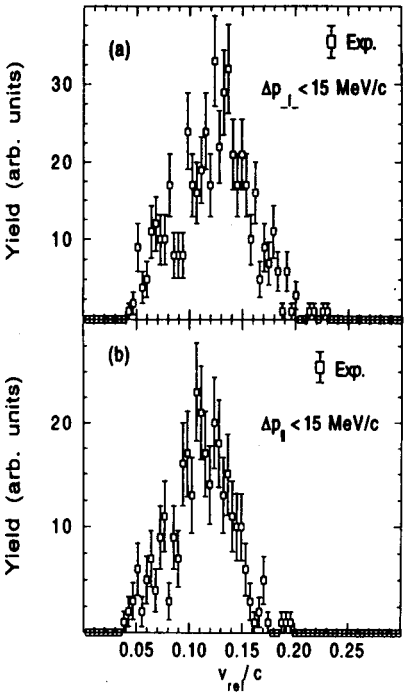

Fig. 6. Distributions of $v_{\rm rel}$ obtained by applying the (a) $\Delta p_\perp \leq 15$ MeV/c and (b) $\Delta p_\parallel \leq 15$ MeV/c cuts to the data.

REFERENCES

[1] R. Hanbury-Brown, R.Q. Twiss, *Phil. Mag.* **45**, 663 (1954).
[2] S.E. Konnin, *Phys. Lett.* **B70**, 43 (1977).
[3] D. Shapira, K. Teh, J. Blankenship, B. Burks, L. Foutch, H.J. Kim, M. Korolija, J.W. McConnell, M. Messick, R. Novotny, D. Rentch, J. Shea, J.P. Wieleczko, *Nucl. Instrum. Methods* **A301**, 76 (1991).
[4] J. Gomez del Campo, R. Stokstad, ORNL Report No TM7295 1981 (unpublished).
[5] M. Korolija, D. Shapira, N. Cindro, J. Gomez del Campo, H.J. Kim, K. Teh, J.Y. Shea, *Phys. Rev. Lett.* **67**, 572 (1991).
[6] M. Korolija, D. Shapira, J. Gomez del Campo, E. Chavez, N. Cindro, *Phys. Rev.* **C49**, 272 (1994).
[7] G.I. Kopylov, *Phys. Lett.* **B50**, 472 (1974).
[8] W.A. Zajc, J.A. Bistirlich, R.R. Bossingham, H.R. Bowman, C.W. Clawson, K.M. Crowe, K.A. Frankel, J.G. Ingersoll, J.M. Kurck, C.J. Martoff, D.L. Murphy, J.O. Rasmussen, J.P. Sullivan, E. Yoo, O. Hashimoto, M. Koike, W.J. McDonald, J.P. Miller, P. Truöl, *Phys. Rev.* **C29**, 2173 (1984).